Design, microfabrication and measurement of cooling arm for fusion energy source application

Shui-Dong Jiang[1,2], Jing-Quan Liu[1,2], Bin Yang[1,2], Hong-Ying Zhu[1,2], Chun-Sheng Yang[1,2]

[1]*Science and Technology on Micro/Nano Fabrication Laboratory, Institute of Micro and Nano Science and Technology, Shanghai 200240, People's Republic of China*
[2]*Institute of Micro and Nano Science and Technology, Shanghai Jiao Tong University, Shanghai 200240, People's Republic of China*
E-mail: jqliu@sjtu.edu.cn

Published in Micro & Nano Letters; Received on 28th June 2013; Revised on 14th August 2013; Accepted on 13th November 2013

The novel cooling arm plays an important role in thermal transfer in the production process of fusion energy. Its structure is designed and simulated by a finite element method. The result shows that the structure with two branches can obtain a temperature difference less than 1 mK among the grip surfaces of all the fingers. A (111) crystal orientation silicon is deployed to fabricate the cooling arm, because of its isotropic Young's modulus. The thermal conductivity of this material is measured by a Gifford-McMahon (GM) cooler. The result shows it has large thermal conductivity at cryogenic temperature, which excellently contributes to heat transfer. The cooling arm is obtained by a microfabrication process. With a uniform pattern width mask and optimised deep reactive ion etching process recipe, a nearly 90° vertical sidewall is obtained. The temperature distribution of the cooling arm is also measured by a GM cooler, and the result shows that the maximum temperature deviation is 0.48 mK among the 16 fingers. There is a good agreement between finite element analysis and the experimental result.

1. Introduction: With the strident development of society, more and more energy will be consumed. Moreover, the energy resources on earth are limited. It is necessary to find an alternative energy to solve this problem. Fusion can generate enough power without negative environmental impacts, such as powder and radiation. Inertial confinement fusion (ICF) is a path to obtain controllable nuclear fusion energy [1, 2]. The ICF energy is generated by heating and compressing a fuel capsule, and it can yield more than the input energy [3]. The fuel material is composed of deuterium and tritium (D-T), which can be directly and indirectly derived from seawater.

The ignition target is the most important part in the ICF experiments. Fig. 1 is the schematic diagram of the target [4]. It mainly contains D-T fuel, a capsule with filled tube, a hohlraum and a thermalmechanical package (TMP). The temperature of the fuel is 18.3 K with a fluctuation limited to less than 1 mK is a necessary condition to produce uniform cryogenic DT layers for the ICF to occur [1, 5]. The TMP contains cooling arms and aluminium sleeves. It is mainly used to support the fusion reactor and obtain the temperature for the fuel. The fusion reactor mainly contains fuel, capsule and hohlraum. The size of this assembly is about Φ5.75 mm × 9.43 mm. The cooling arm is installed at the end of the aluminium sleeve. It plays an important role in heat transfer. To obtain the precise temperature, the temperature difference must be less than 1 mK among the fingers. In this Letter, the structure of the cooling arm is designed and researched. The material selection and the heat transfer characteristics of the cooling arm are also presented.

2. Material selection for the cooling arm: The material to fabricate the cooling arm should have a large thermal conductivity in cryogenic temperature for good thermal transfer. The thermal conductivities of copper and silicon materials are tested by a Gifford-McMahon (GM) , GM-408 cryocooler. The relationship between the thermal conductivity and the temperature is shown in Fig. 2. It is well known that Cu has a large thermal conductivity. However, the test result shows that silicon has a larger thermal conductivity than Cu in the temperature range from 10 to 180 K. From room temperature, the thermal conductivity of silicon rapidly increases by decreasing the temperature. When the temperature arrives at about 20 K for the fusion reaction, the thermal conductivity reaches the maximum value of 2400 W/mK. The (111) crystal orientation silicon has an isotropic Young's modulus [6], which can produce a uniform force in all the fingers when holding the aluminium sleeve. The intrinsic silicon has a large resistivity, and it is also easy to form an oxide to avoid the leads interconnection on the top surface of the cooling arm. Thus, the (111) oriented intrinsic silicon wafer is selected as the material for the cooling arm.

3. Structure design of the cooling arm: The cooling arms with 16 fingers are designed to hold the aluminium sleeve. The fingers are distributed symmetrically at one end of the arm. They grip the aluminium sleeve and flex to compensate for the dimensional changes resulting from cooling the target from room temperature to the cryogenic conditions. The mechanical property of the cooling arm with 16 grip fingers had been researched in our previous Letter [7].

To obtain a temperature fluctuation within 1 mK for the fuel, it is necessary to design a cooling arm with a temperature difference of less than 1 mK among the fingers during heat transfer. To determine the structure (particularly, the number of branches) of the cooling arm and evaluate its heat transfer performance, we have performed thermal modelling of the cooling arm by using the commercial finite element analysis software ANSYS. The models used in ANSYS are designed with no, one and two branches. To make the steady thermal analysis on the proposed thermal models, several assumptions are made. The thermal conductivity of the silicon material is assumed to be constant and isotropic of 2400 W/mK over the temperature range of interest (18–20 K). Convection to air is taken into account. ANSYS lets the user specify convection as a surface load applied to the exposed boundary surfaces. The convection film coefficient here is specified at a constant 5 W/K·m^2, which may be larger than the factual one. Radiation to ambient air has not been taken into account. As a boundary condition, the cooling arm is held at about 1 cm to its

doi: 10.1049/mnl.2013.0407

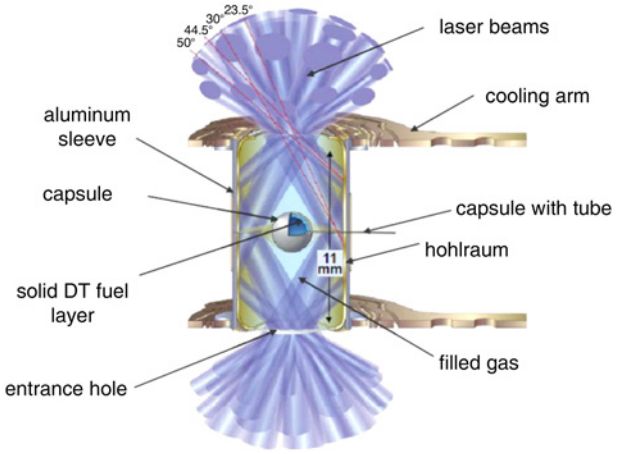

Figure 1 *Schematic diagram of the cryogenic target*

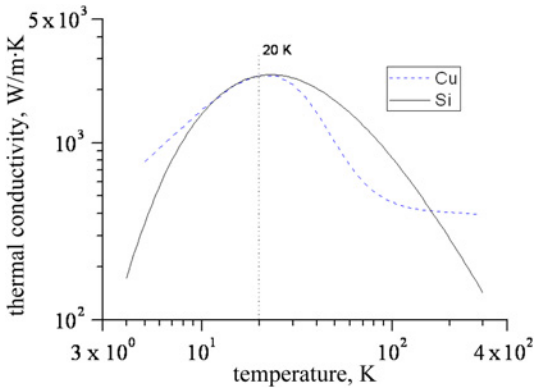

Figure 2 *Thermal conductivity test*

tail end, where the temperature is maintained at a constant 18 K. The ambient temperature is set as 20 K.

Under these conditions, the temperature distributions of the cooling arms with no, one and two branches are presented in Figs. 3*a*–*c*, respectively. It was found that the temperature difference among the grip surfaces of the 16 fingers strongly depends on the number of branches. As shown in Fig. 4, there is a periodic variation of the arm temperature with local maximum and minimum values for all the cooling arm structures, because the fingers are centro-symmetrically distributed on one end of the cooling arm. The maximum values correspond to the long thermal transfer path, and the minimum values correspond to the short thermal transfer path. When there is no branch in the cooling arm, the difference of temperature among the fingers is 2.9 mK which is larger than 1 mK. On the condition of one branch, the difference of temperature among them is 1.39 mK, which exceeds the control level of 1 mK, as well. For two branches, the maximum difference among them is 0.93 mK, which is smaller than 1 mK and is fit for the temperature accuracy requirement. It can be concluded that the temperature difference will decrease with the number of branches increasing. The temperature difference is also affected by the thermal convection. When the convection coefficient is below 5 W/K·m^2, the temperature difference will become small. As shown in Fig. 3*c*, the temperature distributed in the fingers is less than 18.3 K, which can be reached by the heater fixed on the cooling arm. It was verified that the temperature difference is also less than 1 mK, when the heater was used to obtain the temperature 18.3 K of the finger. The conductor layer on the cooling arm is used to electrically connect the sensor and the heater for the temperature control. Thus, the final structure of the cooling arm is shown in Fig. 5.

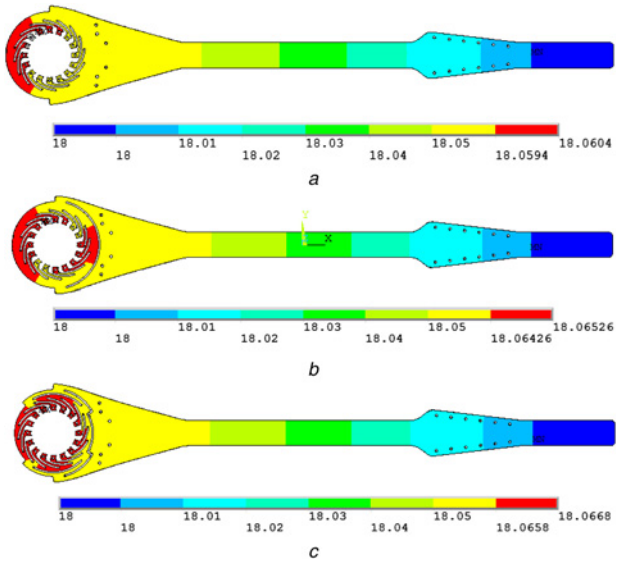

Figure 3 *Temperature distribution of the cooling arm with different structures by finite element method*
a No branch
b One branch
c Two branches

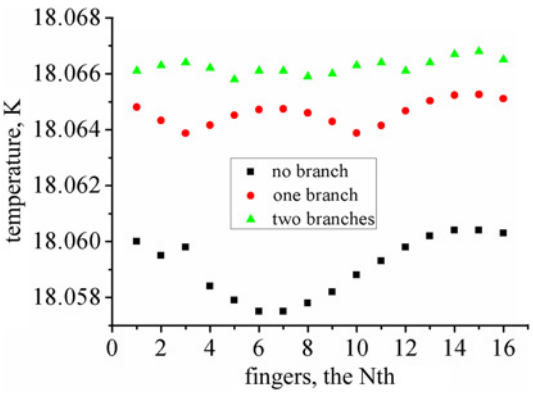

Figure 4 *Temperature difference among the fingers for no branch, one branch and two branches cooling arm*

4. Fabrication of the cooling arm: Fig. 6*a* illustrates the fabrication process flow of the cooling arm. A 500 µm-thick (111) oriented silicon wafer (double-side polished and oxidised) is used as the substrate. The thickness of the oxide layer is 1 µm. In step (1), the SiO_2 layer on the back side of the substrate is removed by reactive ion etching (RIE) for the following through-wafer deep reactive ion etching (DRIE). In step (2), positive photoresist is spin-coated patterned. In step (3), the SiO_2 layer on the top side of the substrate is patterned by RIE to place the thermal sensor and the heater. In steps (4) and (5), the lift-off process is used to form the Cr/Au (20/150 nm) conductor layer. The layer is prepared by a magnetron sputter on top of the SiO_2 layer, and it is used to connect the sensor and the heater. In step (6), to form the cooling arm structure, approximately 20 µm positive photoresist is spin-coated and patterned on top of the

Figure 5 *Final structure of the cooling arm*

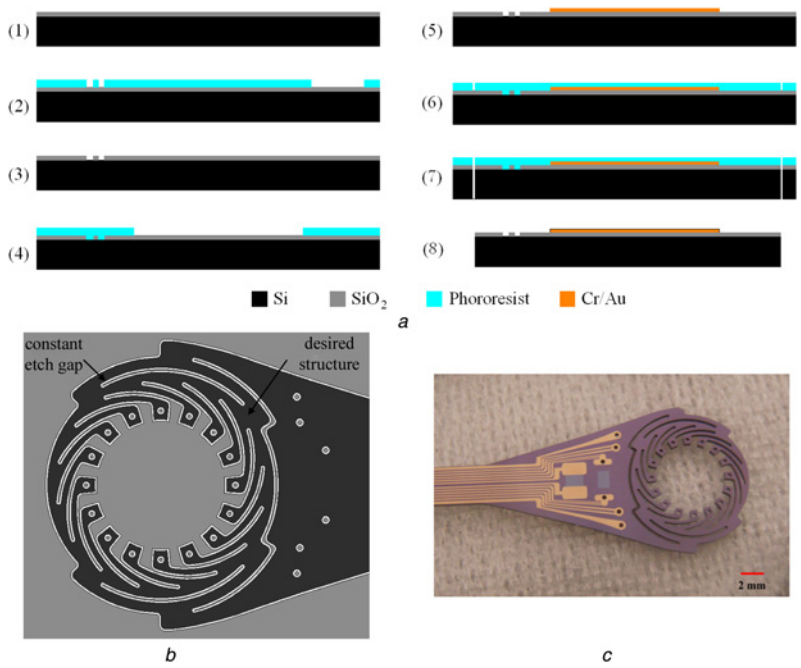

Figure 6 *Graph for the cooling arm*
a Fabrication-process flow
b Mask with constant channel width
c Picture of the fabricated cooling arm

wafer for the through-wafer etching. The mask for the DRIE is designed with a uniform width geometry with all the etching occurring in a constant-width trench of 80 μm, as shown in Fig. 6*b*. This can avoid the lag effect, obtain the same sidewall morphology and achieve the high vertical sidewall [8–12]. The high sidewall vertical degree of the fingers will obtain a large contact area between the cooling arm and the aluminium sleeve, which will contribute obtaining stable gripping and good heat transfer. In step (7), the SiO_2 layer on the top side of the substrate is patterned by RIE. The patterned SiO_2 and the photoresist layers are used to act as the mask of DRIE. The parameters of the DRIE are optimised to obtain a high sidewall vertical degree [13–16], as shown in Table 1. In each cycle, the passivation time is reduced and the etch time is raised. Finally, the through-wafer DRIE was finished. In step (8), the photoresist is removed in acetone and IPA. Finally, the picture of the fabricated cooling arm is shown in Fig. 6*c*.

Table 1 Optimised parameters of DRIE (Versaline-LL ICP-DSE)

	Passivation time, s	Etch time, s
un-optimised	5	5
optimised	3	7

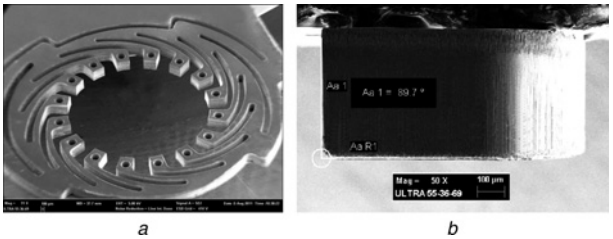

Figure 7 *View of*
a DRIE etch of the cooling arm
b Vertical etch profile

5. Sidewall measurement: The cooling arm is fabricated, and it provides segments for profile view in a scanning electron microscope (SEM). The image of the complex part of the cooling arm is shown in Fig. 7*a*. The SEM image of part of the cooling

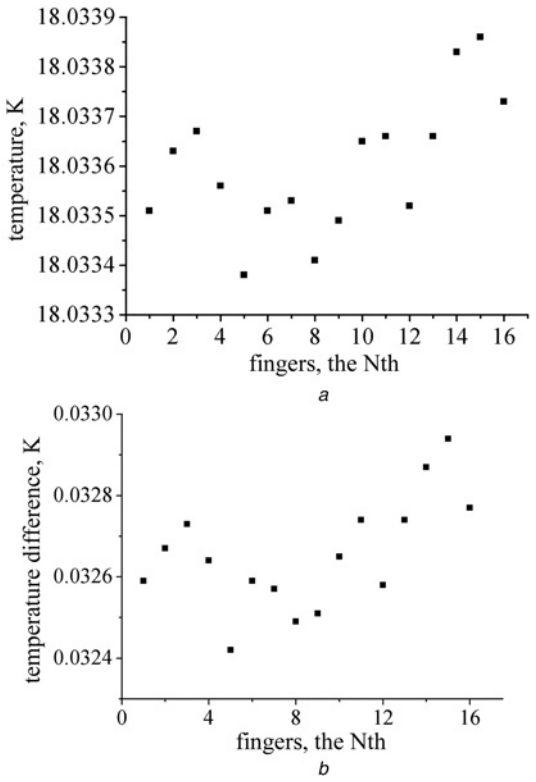

Figure 8 *Temperature distribution measurement and temperature difference*
a Temperature distribution measurement
b Temperature difference between the simulation and the experimental result for two branches cooling arm

doi: 10.1049/mnl.2013.0407

arm allowed measurement of the sidewall vertical degree. The sidewall vertical degree refers here to the angle between the cooling arm top or down surface and the etched sidewall of the cooling arm. As shown in Fig. 7*b*, it has a high sidewall vertical degree, and the averaged angle is within $90 \pm 0.5°$.

6. Temperature distribution measurement: The temperature distribution of the cooling arm was measured in cryogenic temperatures by a GM cooler, cryogenic temperature controller (Cryocon) 24C and resistance temperature sensors. The GM cooler provided 18 K temperature and an ambient temperature for the cooling arm. Cryocon 24C was used to obtain the temperature value of the sensors. The sensors were deployed to measure the temperature on the grip surfaces of the cooling arm, and each temperature sensor was connected with the Cryocon 24C by four leads. During the test, 1 cm to its tail end of the cooling arm was held with a temperature of 18 K, and the rest of it was exposed in 20 K ambient air. 16 CERNOX-1050 temperature sensors were distributed on the 16 finger tips, respectively. They were used to measure the temperature distribution of the 16 finger tips. The epoxy has an excellent low temperature thermal conductivity, and the temperature sensors were fixed on the grip surface by it before the temperature measurement. The test result is shown in Fig. 8*a*. It can be seen that the temperature difference among the 16 fingers is 0.48 mK less than 1 mK, which is in good agreement with the result of the finite element method. It can meet the temperature accuracy of the shaped fuel. As shown in Fig. 8*b*, the temperature difference between the simulation and the experimental result is in the 0.03242–0.03294 K range. The temperature value and the temperature difference are less than the result of the finite element method. It should be noted that the convection coefficient was less than 5 $W/K{\cdot}m^2$ during measurement. As the ambient temperature is higher than the temperature of the cool end, the temperature value and the temperature difference of the fingers will decrease with decreasing convection coefficient.

7. Conclusion: In summary, a novel cooling arm was developed to grip and transfer heat from the aluminium sleeve for the first time to our knowledge. Silicon material was used to fabricate a cooling arm with large thermal conductivity of 2400 W/mK in cryogenic temperatures about 20 K. The cooling arm with no, one and two branches were designed. The temperature distribution of the three structures was simulated by the finite element method. The results show that the two branches structure can obtain a temperature difference of 0.93 mK among the fingers. It can meet the temperature accuracy of less than 1 mK of the shaped fuel. The cooling arm was obtained by a microfabrication process. By using a mask with a constant-width trench of 80 μm, the fabricated cooling arm had a high vertical sidewall with an approximate angle of $90 \pm 0.5°$. The high vertical sidewall will form a maximum contact area between the cooling arm and the aluminium sleeve, and it is good for thermal transfer between them. The temperature distribution of the cooling arm was also measured by a GM cooler. The test result shows that the temperature difference among the fingers is 0.48 mK, and as it is less than 1 mK, it is in good agreement with the result of the finite element method. The difference between them is caused by the different convection coefficients. Thus, the designed and fabricated cooling arm with two branches is a good fit for thermal transfer in the production process of fusion energy.

8. Acknowledgments: This work was partly supported by the National Natural Science Foundation of China (no. 61076107), the Shanghai Municipal Science and Technology Commission (nos. 11DZ2290203 and 11JC1405700), Program for New Century Excellent Talents in University (2009). The authors also thank Professor Yong-Hua Huang for his essential contribution to this work.

9 References

[1] Moses E.I.: 'Ignition on the National Ignition Facility: a path towards inertial fusion energy', *Nucl. Fusion*, 2009, **49**, (10), p. 104022
[2] Lindl J.: 'Development of the indirect-drive approach to inertial confinement fusion and the target physics basis for ignition and gain', *Phys. Plasmas*, 1995, **2**, (11), pp. 3933–4024
[3] Glenzer S.H., Collahan D.A., Mackinnon A.J., *ET AL.*: 'Cryogenic thermonuclear fuel implosions on the National Ignition Facility', *Phys. Plasmas*, 2012, **19**, (5), p. 056318
[4] Moses E.I.: 'The National Ignition Facility (NIF): a path to fusion energy', *Energy Convers. Manage.*, 2008, **49**, (7), pp. 1795–1802
[5] Moses E.I.: 'Ignition on the National Ignition Facility'. Proc. Fifth Int. Conf. on Inertial Fusion Sciences and Applications, Kobe, Japan, 2008, p. 012003
[6] Kim J., Cho D., Muller R.: 'Why is (111) silicon a better mechanical material for MEMS'. Proc. Transducers 2001, Munich, Germany, 2001, **8**, pp. 662–665
[7] Jiang S.-D., Liu J.Q., Yang B., Zhu H.-Y., Yang C.-S.: 'Microfabrication of cooling arm for fusion energy source application', *Micro Nano Lett.*, 2013, **8**, pp. 181–183
[8] Pike W., Karl W.J., Kumar S., *ET AL.*: 'Analysis of sidewall quality in through-wafer deep reactive-ion etching', *Microelectron. Eng.*, 2004, **73**, pp. 340–345
[9] Jansen H., Gardeniers H., de Boer M., ELwenspoek M., Fluitman J.: 'A survey on the reactive ion etching of silicon in microtechnology', *J. Micromech. Microeng.*, 1996, **6**, (1), pp. 14–28
[10] Ikehara T., Maeda R.: 'Fabrication of an accurately vertical sidewall for optical switch applications using deep RIE and photoresist spray coating', *Microsyst. Technol.-Micro Nanosyst.-Inf. Storage Process. Syst.*, 2005, **12**, (1–2), pp. 98–103
[11] Ganji B.A., Majlis B.Y.: 'Fabrication of deep trenches in silicon wafer using deep reactive ion etching with aluminum mask', *Sains Malaysiana*, 2009, **38**, (6), pp. 889–894
[12] Chung C.K.: 'Geometrical pattern effect on silicon deep etching by an inductively coupled plasma system', *J. Micromech. Microeng.*, 2004, **14**, (4), pp. 656–662
[13] Ohara J., Takeuchi Y., Sato K.: 'Improvement of high aspect ratio Si etching by optimized oxygen plasma irradiation inserted DRIE', *J. Micromech. Microeng.*, 2009, **19**, (9), p. 095022
[14] Juan W.H., Pang S.W.: 'High-aspect-ratio Si etching for microsensor fabrication', *J. Vac. Sci. Technol. A, Vac. Surf. Films*, 1995, **13**, (3), pp. 834–838
[15] Agarwal R., Samson S., Bhansali S.: 'Fabrication of vertical mirrors using plasma etch and KOH: IPA polishing', *J. Micromech. Microeng.*, 2007, **17**, (1), pp. 26–35
[16] Aachboun S., Ranson P.: 'Deep anisotropic etching of silicon', *J. Vac. Sci. Technol. A*, 1999, **17**, (4), pp. 2270–2273